

Study on Preparation and Swelling Kinetics of P(AA-co-C₈PhEO₁₀Mac) pH-Sensitive Hydrogel *In Vitro* Drug Release Study

Fang Ping Wang, Hu Po Mu, Jun Yin Zhang, Wan Xia Li, Qi Zhao Wang, Xin Zhen Du

Key Laboratory of Eco-Environment-Related Polymer Materials, Ministry of Education of China, College of Chemistry and Chemical Engineering, Northwest Normal University, Lanzhou 730070, China

Correspondence to: F. P. Wang (E-mail: wangfp@nwnu.edu.cn)

ABSTRACT: Stimuli-sensitive hydrogels are one of the most promising and versatile materials with many potential applications. In this article, a pH-sensitive hydrogel [P(AA-co-C₈PhEO₁₀Mac)] was synthesized by the free-radical cross-linking polymerization of acrylic acid (AA) and octylphenyl polyoxyethylene methacrylate macromonomer (C₈PhEO₁₀Mac). Swelling property, swelling, and deswelling kinetics of the hydrogels in different pH media were studied and hydrogel microstructures were investigated by means of scanning electron microscopy (SEM). Theophylline was chosen as a model drug and the controlled-release properties of hydrogels were pilot studied. The results showed that the P(AA-co-C₈PhEO₁₀Mac) hydrogel has a porous structure, both the rapid swelling and deswelling rate, and good pH sensitivity characteristics; The swelling ratios of the gels in stimulated intestinal fluids (SIF, pH = 7.4) were higher than those in stimulated gastric fluids (SGF, pH = 1.4). The *in vitro* cumulative release data were analyzed using an empirical equation to compute the diffusion exponent (*n*), whose values suggest a non-Fickian mode of transport. © 2013 Wiley Periodicals, Inc. *J. Appl. Polym. Sci.* 130: 1981–1989, 2013

KEYWORDS: drug delivery systems; kinetics; swelling; biomaterials; cross-linking

Received 11 November 2012; accepted 6 April 2013; Published online 13 May 2013

DOI: 10.1002/app.39388

INTRODUCTION

Stimuli-responsive hydrogels have been produced that exhibit dramatic changes in their swelling behavior, network structure, permeability, and mechanical strength in response to a number of external stimuli, such as pH, ionic strength of the surrounding fluid, temperature, presence of specific solutes, as well as applied electrical and magnetic fields.¹ Because of their nature, these materials can be used in a wide variety of applications, such as separation, biosensors, tissue engineering,² and drug delivery devices.^{3–5} In all of their applications, the controlled drug delivery is the most prominent area.⁶ The smart hydrogels are useful in the controlled drug delivery because the swelling process is slow,⁷ the drug delivery is to obtain a constant release rate for a prolonged time, and the release kinetics can simultaneously be controlled.⁸ In fact, they have been employed to target-release a drug or protein to a specific site in the body.

pH-sensitive hydrogels, owing to the fact that they can conventionally change their volume in response to environment stimuli with different pH, had been widely used in the area of drug delivery system.^{9–13} These polymers include chitosan,¹⁴ methacrylic acid or hydroxyethyl methacrylate,¹⁵ azo-aromatic polymers,¹⁶ methacrylated inulin,¹⁷ cellulose derivatives such as ethyl cellulose,¹⁸ hydroxypropyl methylcellulose acetate

succinates, cellulose acetate phthalate,¹⁹ cellulose acetate butyrate,²⁰ as well as pectin and its salts.²¹ But a fatal shortcoming of traditional hydrogel is the slow response speed, therefore, in recent years much more attention has been directed to improving the response rate of intelligent gels.

Theophylline is a naturally occurring 1,3-dimethylxanthine alkaloid known for the extensive pharmacological actions, such as relaxing tracheal smooth muscle, exciting respiratory center, increasing myotility of diaphragmatic muscle as well as cardio-kinetic and diuretic action, and lowering pulmonary angiotasis. Theophylline are still the first-line antiasthmatic drugs prescribed in the clinic of some countries, but the drug has dose-related side effects (>20 µg/mL) such as nausea, ulcers, cardiac arrhythmia, and epigastric pain.²² Hence, developing a controlled release formulation of theophylline would minimize the dosing frequency and side effects. In this study, a pH-sensitive P(AA-co-C₈PhEO₁₀Mac) hydrogel was successfully prepared using acrylic acid (AA) and C₈PhEO₁₀Mac as monomers in the presence of a cross-linker, *N,N*-methylenebisacrylamide. The swelling behavior was probed and the theophylline release rate has been evaluated by performing *in vitro* studies in simulated gastric and intestinal fluids. The advantages of the hydrogel are shorter swelling equilibrium time, fast response rate, good pH

reversibility after multiple cycling, and suitability for the release of theophylline in the intestinal tract. The only disadvantage of the hydrogel is shorter drug release time. The resulting copolymer hydrogels are expected to be utilized in tissue engineering materials and drug control delivery fields as a potential biomaterial.

EXPERIMENTAL

Materials and Methods

AA (99.5%) and methacryloyl chloride (99%) purchased from Tianjin Kaixin Chemicals (China) were used after distillation. Octylphenol polyoxyethylene ether (C_8PhEO_{10} , 98%) purchased from Tianjin Fuchen Chemicals (China) was used as received. *N,N*-methylenebisacrylamide (BIS, 98%) purchased from Shanghai Zhongxin Chemicals (China). Ammonium persulfate (APS, 98%) was acquired from Yantan Shuanghua Chemicals (China). Sodium bisulfite (SBS, 98%) acquired from Qingdao Shuanglongteng Chemicals (China) were recrystallized before use. Buffer solutions with different pH values of 1.4, 3, 5, 7.4, 9, 11, and 13 as physiological mediums were freshly prepared with HCl, $Na_2HPO_4 \cdot 12H_2O$, $NaH_2PO_4 \cdot 2H_2O$, $NaB_4O_7 \cdot 10H_2O$, Na_2CO_3 , $NaHCO_3$, and $Na_3PO_4 \cdot 12H_2O$ in order to examine the swelling behavior, and NaCl was used to adjust the ionic intensities. Theophylline purchased from Aldrich was used as a model drug.

C₈PhEO₁₀Mac Preparation

$C_8PhEO_{10}Mac$ was prepared with C_8PhEO_{10} and methacryloyl chloride in toluene. C_8PhEO_{10} (27.5 mmol), triethylamine (49.4 mmol), and toluene (80 mL) were charged into a 250 mL, three-necked, round-bottom flask equipped with a dropping funnel, thermometer, and water condenser. The resulting reaction mixture was cooled in an ice bath, and the temperature was maintained in the range 0–7°; then, methacryloyl chloride (27.5 mmol) was added in a dropwise manner. After the completion of the addition, the reaction mixture was warmed to room temperature and was continuously stirring for 24 h. After the solvent was removed, the residue was purified by column chromatography with 3:1 ethyl acetate/petroleum ether as the eluent. In the following text, $C_8PhEO_{10}Mac$ was denoted as CM, for simplification.

Hydrogels Preparation

P(AA-*co*- $C_8PhEO_{10}Mac$) hydrogels were synthesized by free-radical cross-linking copolymerization of $C_8PhEO_{10}Mac$ and AA in aqueous solutions. A stoichiometric monomer (mass ratios of $C_8PhEO_{10}Mac$ to AA were 1:10, 1:20, 1:30, and 1:40) was dissolved in 7 mL ultra-pure water. Later, BIS (BIS as cross-linking agent was used at 1.5 wt % with respect to the total amount of monomers) was added into the monomer mixture. The mixture solution was bubbled with nitrogen for 30 min to remove the dissolved oxygen. After the stirring proceeded at 40°C for about 10 min, the APS and SBS (APS and SBS were used as initiators in 2:1 wt ratio, at concentrations of 0.4 wt %, each of them with respect to the total amount of monomers) were added into the reaction mixture accompanied by rapid stirring at 40°C for another 8 h. The products were flushed with ultra-pure water for 7 d, and the water was refreshed everyday in order to remove the unreacted monomers and cross-linking agents.

Finally, hydrogels were dried in an oven at 40°C until constant weight.

Measurements and Characterization

FT-IR spectra of the hydrogel sample and the macromonomers were recorded on FTS 3000 spectrometer (DIGILAB, USA). Aliquots were withdrawn periodically and analyzed using a UV-Vis spectrophotometer (Agilent 8453, Japan). SEM was employed to investigate the morphology of P(AA-*co*- $C_8PhEO_{10}Mac$) hydrogel. The hydrogels were immersed in pHs of 1.4 and 7.4, and were frozen in liquid nitrogen and lyophilized for 24 h. Then, the hydrogels were sputtered with gold before observation. In this study, morphology of prepared particles was examined on JEOL SEM (JSM-5600LV, JEOL, and Japan).

Swelling Measurement

A classical gravimetric method was used to measure the swelling ratio of hydrogel at 37°C. The dried hydrogels (W_0) were immersed in an excess amount of buffer solutions of 1.4, 3, 5, 7.4, 9, 11, and 13, respectively at 37°C. The wet weight of the samples (W_t and W_e) was determined after removing the surface water by blotting with filter paper. Taking the average value of three measurements for each sample, the swelling ratio (R) and the equilibrium swelling ratio (R_e) were calculated according to the following equation³:

$$R = \frac{W_s - W_d}{W_d} \quad R = (W_s - W_d) / W_d \quad (1)$$

$$R_e = \frac{W_e - W_d}{W_d} \quad (2)$$

where W_d and W_s are the weights of dry and swollen hydrogels, respectively. W_e denote the weight of the hydrogels at equilibrium swelling.

Determination of Loading and Encapsulation Efficiency

The drug-loaded hydrogels (30 mg) were submerged in 50 mL SIF as release environment. The temperature was kept at 37°C for 12 h and the stirring rate was maintained at 100 rpm. The amount of released theophylline analyzed using a UV-Vis spectrophotometer. The wavelength of maximal absorbance for theophylline was set at 270 ± 1 nm. The loading efficiency (LE) and encapsulation efficiency (EE) were calculated according to the following equation²³:

$$LE(\%) = \frac{W_1}{W_d} \times 100 \quad (3)$$

$$EE(\%) = \frac{W_1}{W_2} \times 100 \quad (4)$$

where W_1 and W_2 are total amount of theophylline in hydrogel and total amount of used theophylline, respectively, W_d is the gel weight.

In Vitro Drug Delivery Study

The drug-loaded and released properties were evaluated by using theophylline as drug target. The dried P(AA-*co*- $C_8PhEO_{10}Mac$) was immersed in the drug target aqueous solution (5 g/L) for 7 d

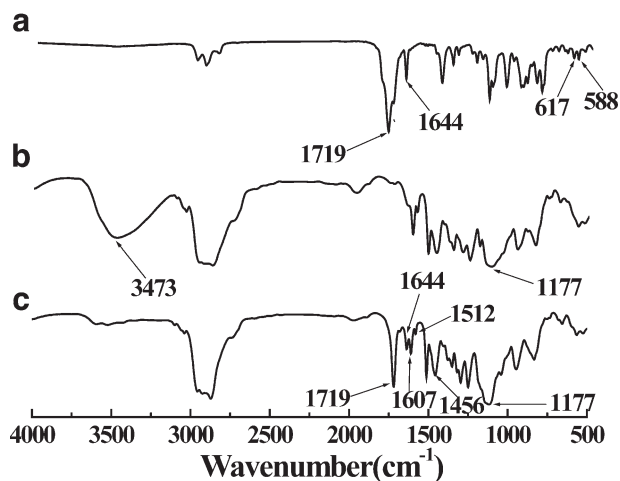


Figure 1. FT-IR spectra of C₈PhEO₁₀Mac (a), AA (b) and P(AA-*co*-C₈PhEO₁₀Mac) (c) hydrogel.

at room temperature. The drug-loaded hydrogels were rinsed with distilled water and dried until a constant weight under vacuum was achieved. After that, the samples were submerged in 50 mL SGF and SIF as release environment. The temperature was kept at 37°C and the stirring rate was maintained at 100 rpm. Aliquots from the dissolution medium were withdrawn periodically and analyzed using a UV-Vis spectrophotometer. The wavelength of maximal absorbance for theophylline was set at 270 ± 1 nm. The cumulative drug release was calculated from the following relationship²⁴:

$$\text{Cumulative release (\%)} = \frac{M_t}{M_0} \times 100 \quad (5)$$

where M_t is the amount of drug released from hydrogels at time t , and M_0 is the amount of drug loaded into the hydrogels. Here, M_0 was estimated by subtracting the amount of unloaded drug from the feed drug.

RESULTS AND DISCUSSION

FT-IR Spectra

The IR spectrum of P(AA-*co*-C₈PhEO₁₀Mac) hydrogel is shown in Figure 1(c). The absorption peaks at 1729 cm⁻¹ (C=O) for the carbonyl group; 1455, 1512 cm⁻¹ for the phenyl group (C=C) stretching vibration band; 1107 cm⁻¹ doublets were assigned to the symmetric C—O—C stretching modes of the ester group; compared to the IR spectrum of C₈PhEO₁₀Mac [Figure 1(a)], a new stretching vibration band at 3429 cm⁻¹ of hydroxyl group (—OH) appeared, and the out-of-plane bending band at 990 cm⁻¹ for unsaturated hydrocarbons (C—H) disappeared. These provided evidence for the successful copolymerization of AA and C₈PhEO₁₀Mac.

pH Dependence of Degree of Swelling

Figure 2 shows typical equilibrium swelling curves of P(AA-*co*-C₈PhEO₁₀Mac) hydrogels. With increased phosphate buffer solution pH from 1.4 to 9, the swelling capacity increases because the carboxyl (—COOH) in P(AA-*co*-C₈PhEO₁₀Mac) exists as —COO⁻. With increased pH of solution from 9 to 13, the degree of swelling decreases gradually because the hydrogels would form

more ionic bonds between P(AA), which results in the relative increased cross-linking density of the hydrogel. The hydrogels exhibit lower swelling capability in an acid medium and higher swelling degree in a basic medium. This is related to the fact that the carboxyl groups as functional groups could accept or release protons in response to various pH aqueous media. A lot of hydrogen bonds were formed because of the presence of carboxyl groups in the gel networks in acid surroundings. The hydrogen bond interaction would restrict the movement or relaxation of the gel network chains. As a result, a compact hydrogel network was formed, leading to a lower swelling ratio. On the contrary, in neutral or alkaline media, these free carboxylic acid groups would be ionized to free ions. Consequently, hydrogen bonds were broken and an electrostatic repulsion was generated among polymer networks. This repulsive force would push the network chain segments apart and thus attract more water into the hydrogels, so a higher swelling ratio was observed. Carboxyl ionization reaches a maximum extent when pH = 9 and the pH continues to increase as the hydrogel networks are deswelled or shrunk. It is attributed to the “charge screening effect” of the anions on the polymer network leading to the reduction of osmotic pressure.

Ionic Strength Dependence of the Swelling Degree

The influences of different ionic strength on the swelling degree of hydrogels is shown in Figure 3. There is the same decreasing tendency for the degree of swelling of the polyelectrolyte hydrogels in NaCl-buffer solutions with ionic strength increase. As we increase the salt concentration, H⁺ ions in the gel will be exchanged to Na⁺ cation. The ion swelling pressure will increase because of the increasing production of free counterions by dissociation of AA. Therefore, the hydrogel networks are deswelled or shrunk into more compact structures, which makes the diffusion of small molecular ions into the hydrogel networks difficult, leading to a lower osmotic pressure and then a lower swelling ratio.

Swelling Kinetics in SGF and SIF

In order to examine the swelling ability of the P(AA-*co*-C₈PhEO₁₀Mac) hydrogels in harsh environments of the stomachs and the intestines, we prepared several stimulated gastric and intestinal fluids. Considering the temperatures of human

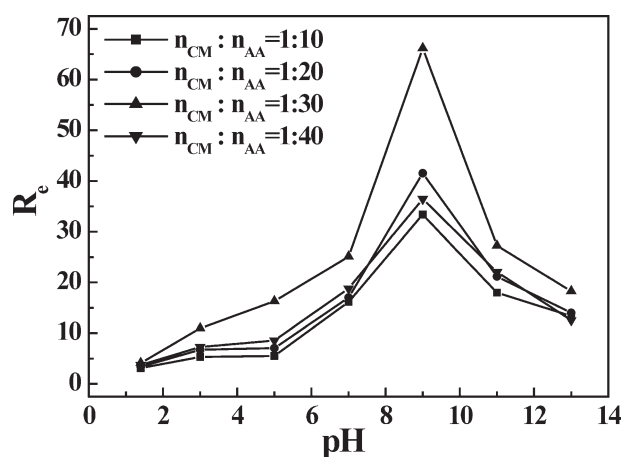


Figure 2. Equilibrium swelling ratios of various P(AA-*co*-C₈PhEO₁₀Mac) hydrogel samples as functions of solution pH values for various samples in buffer solution (Mean ± SD, $n = 3$).

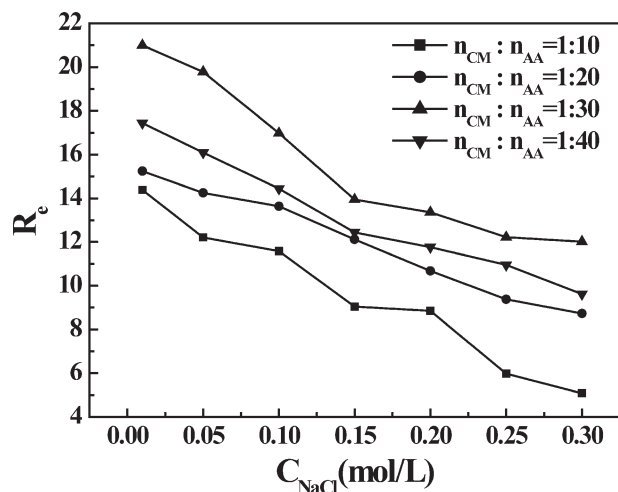


Figure 3. Effect of ionic strength on the degree of swelling of the P(AA-co-C₈PhEO₁₀Mac) hydrogels (Mean \pm SD, $n = 3$).

bodies, the desiccated gels were incubated in the stimulated fluids at 37°C, so as to be suitable for drug controlled release. It could be clearly illustrated from Figure 4 that the swelling ratios of the gels were low in the stimulated gastric buffer fluid, whose maximal value is 5.29, while the ratios in the intestines were higher than those in the stomach for the same swelling time. For instance, the ratios of four samples in the SIF reached 24–38 within 580 min, exhibiting an excellent swelling ability, compared with those in the above SGF, as shown in Figure 4(b). This is ascribed to the fact that the carboxyl groups are ionized into carboxylic ions ($-\text{COO}^-$) in basic conditions of the SIF. The outstanding trait is expected to be utilized in drug controlled release fields. With an increase ratio of C₈PhEO₁₀Mac to AA, the swelling ratios of gels increased, when the ratio reached to 1:40, the swelling ratios began to decrease. When the ratio of C₈PhEO₁₀Mac to AA was 1:30, the swelling ratio was biggest.

This characteristic of P(AA-co-C₈PhEO₁₀Mac) hydrogels is beneficial to the drug controlled release, especially to the drug absorption in intestines instead of in the stomach. When the gels incubated in the intestine surroundings started to swell, the drugs were released into the intestine media.

It is clear that when hydrogel is brought into contact with water, water diffuses into the hydrogel, and the hydrogel swells. Diffusion involves the migration of water into preexisting or dynamically formed spaces among hydrogel chains, while swelling of the hydrogel involves a larger scale segmental motion, resulting ultimately in an increase in the separation distance among the hydrogel chains. To investigate the diffusion mechanism in the gel, the initial swelling data were fitted to eq. (6) for $S/S_\infty \leq 0.6$ ²⁵ as follows:

$$F - \frac{S}{S_\infty} = kt^n \text{ or } \ln(F) = \ln k + n \ln t \quad (6)$$

where F denotes the water fraction at time t , S and S_∞ represent the amount of water absorbed by the hydrogel at time t and at an equilibrium state, respectively, k is a characteristic constant of the hydrogel, and n is a characteristic exponent of

the swelling which represents solvent diffusion modes inside hydrogels, and provides information about the mechanism of swelling kinetics. The constant n and k can be calculated from the slope and intercept of the formula (6). Figure 5 can be used to elucidate dependence of $\ln(F)$ on $\ln(t)$ for various hydrogel samples in SGF and SIF environments. After having been fitted, the kinetic parameters k and n as well as the correlation coefficient R^2 obtained are tabulated in Table I. In an acidic medium (SGF), the equivalent n values (~ 0.5 or below 0.5) for all the samples manifest that the diffusion behavior of water in these hydrogels follows the Fickian mechanism. In the case of a more basic medium (SIF), the swelling index n values are evidently over 0.5, which represents a non-Fickian diffusion.²⁶

The initial swelling process exhibits Fickian behavior, and the extensive swelling process follows the Schott second-order dynamic equation⁸:

$$\frac{dS}{dt} = k_s(S - S_\infty) \text{ or } \frac{t}{S} = A + Bt \quad (7)$$

The constant $B = 1/S_\infty$ and $A = 1/k_s S_\infty^2 = 1/(dS/dt)_0$ can be calculated from the slope and intercept of the formula (7). The function relations of t/S versus t are plotted in Figure 6. The

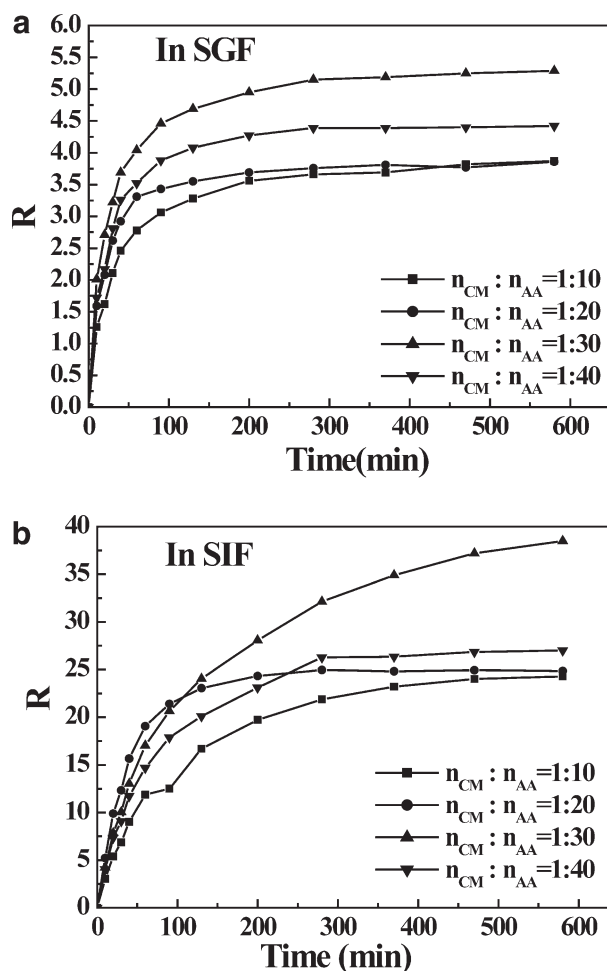


Figure 4. Influence of the composition of P(AA-co-C₈PhEO₁₀Mac) hydrogels on swelling ratios in SGF (a) and SIF (b) at 37°C (Mean \pm SD, $n = 3$).

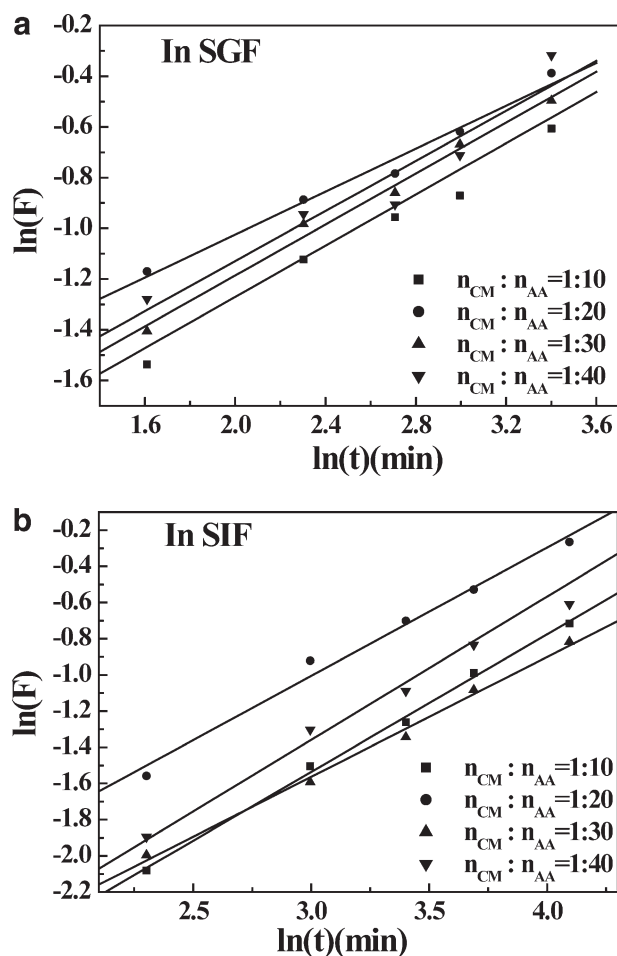


Figure 5. The $\ln F$ versus $\ln t$ curves of P(AA-co-C₈PhEO₁₀Mac) hydrogels in pH = 1.4 (a) and 7.4 (b) buffer solutions at 37°C (Mean \pm SD, $n = 3$).

swelling kinetic equations, k_s , τ_0 , and S_∞ values of hydrogel samples are tabulated in Table II. All the R^2 are greater than 0.99, indicating a small estimated standard error and a highly precise linear regression equation.

Reversible Response of the Gels in different pH Solutions

Considering the discrepancy in the acidic degree of the stomach (pH = 1.4) and intestine (pH = 7.4) in a drug delivery system, a desirable reversible phase transition with the change in

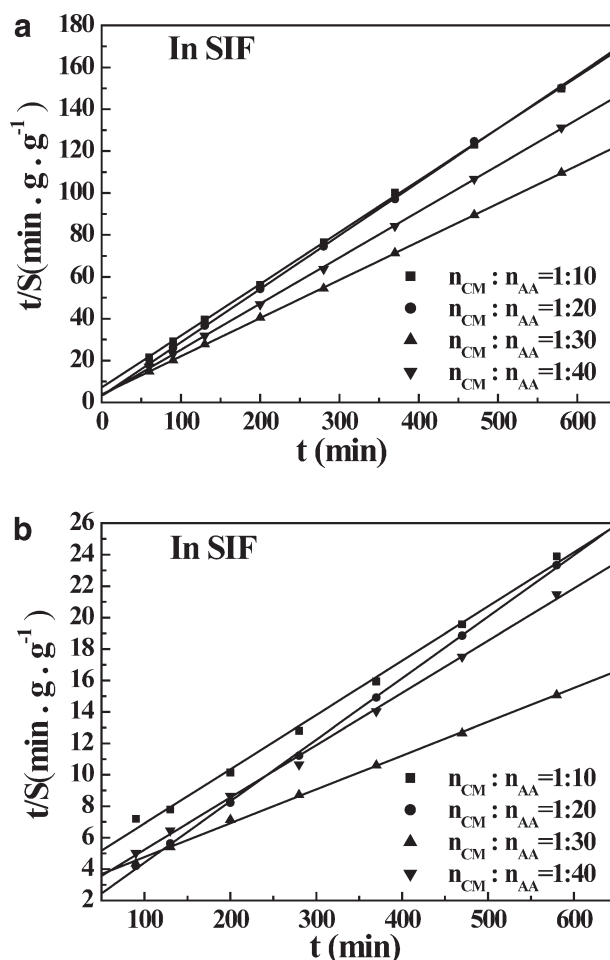


Figure 6. The t/S versus t curves of P(AA-co-C₈PhEO₁₀Mac) hydrogels in pH = 1.4 (a) and 7.4 (b) buffer solutions at 37°C (Mean \pm SD, $n = 3$).

environmental pH is more important. For this reason, a reversibility of the swelling and deswelling behavior was demonstrated by repeatedly cycling P(AA-co-C₈PhEO₁₀Mac) hydrogel samples in stimulated buffers of pH = 1.4 and pH = 7.4 (Figure 7). These experimental results hint that the hydrogels are provided with a relatively fast expansion rate in alkaline surroundings, whereas they shrink as soon as they are immersed into acidic solutions. The phenomena can be explained by the dissociation and formation of an ionic bond between $-\text{COO}^-$ groups in an

Table I. Swelling Kinetic Equations and Kinetic Parameters of P(AA-co-C₈PhEO₁₀Mac) Hydrogel Samples in pH = 1.4 (SGF) and 7.4 (SIF) Buffer Solutions at 37°C (Mean \pm SD, $n = 3$)

Medium	$n_{\text{CM}}:n_{\text{AA}}$	Initial regression equation	R^2	n	$\ln k$
SGF	1:10	$\ln F = 0.4997 \ln t - 2.3195$	0.9890	0.4997	-2.3195
	1:20	$\ln F = 0.4234 \ln t - 1.8716$	0.9822	0.4234	-1.8716
	1:30	$\ln F = 0.5025 \ln t - 2.1911$	0.9907	0.5025	-2.1911
	1:40	$\ln F = 0.4938 \ln t - 2.1169$	0.9215	0.4938	-2.1169
SIF	1:10	$\ln F = 0.7609 \ln t - 3.8186$	0.9973	0.7609	-3.8186
	1:20	$\ln F = 0.7096 \ln t - 3.1340$	0.9867	0.7096	-3.1340
	1:30	$\ln F = 0.6627 \ln t - 3.5510$	0.9943	0.6627	-3.5510
	1:40	$\ln F = 0.7172 \ln t - 3.5098$	0.9925	0.7172	-3.5098

Table II. Extensive Swelling Kinetic Equations, Initial Swelling Rates (r_0), and Maximum Theoretical Water Contents (S_∞) of P(AA-co-C₈PhEO₁₀Mac) Hydrogel Samples in pH = 1.7 (SGF) and 7.4 (SIF) Buffer Solutions 37°C (Mean ± SD, $n = 3$)

Medium	$n_{CM}:n_{AA}$	Extensive regression equation	R^2	S_∞	r_0	k_s
SGF	1:10	(t/s) = 0.2584 t + 7.1467	0.9997	3.87	0.1399	0.009343
	1:20	(t/s) = 0.2590 t + 3.1792	0.9998	3.86	0.3145	0.021111
	1:30	(t/s) = 0.1890 t + 3.8415	0.9999	5.29	0.2603	0.009302
	1:40	(t/s) = 0.2262 t + 3.2073	0.9998	4.42	0.3118	0.015959
SIF	1:10	(t/s) = 0.0412 t + 3.4519	0.9963	24.28	0.2897	0.000494
	1:20	(t/s) = 0.0402 t + 0.4926	0.9998	24.85	2.0301	0.000484
	1:30	(t/s) = 0.0259 t + 0.4927	0.9989	38.49	2.0296	0.000263
	1:40	(t/s) = 0.0370 t + 1.9100	0.9977	27.00	0.5236	0.000712

alkalescent solution and —COOH in an acidic solution. As shown in Figure 7 and Scheme 1, —COOH groups in polymer networks were ionized at a high pH value, resulting in the breakage of hydrogen bonds and thus producing an electrostatic repulsion among gel networks. Meanwhile, the osmotic pressure inside the hydrogels increased, and electrostatic repulsion caused the network to expand. On the other hand, —COO[−] groups can be integrated with H⁺ ions into —COOH groups, which is in favor of the formation of hydrogen bonds and therefore generates an electrostatic repulsion. As a result, the network porosity of these hydrogels changed, and sudden or gradual changes in their equilibrium swelling behavior happened.

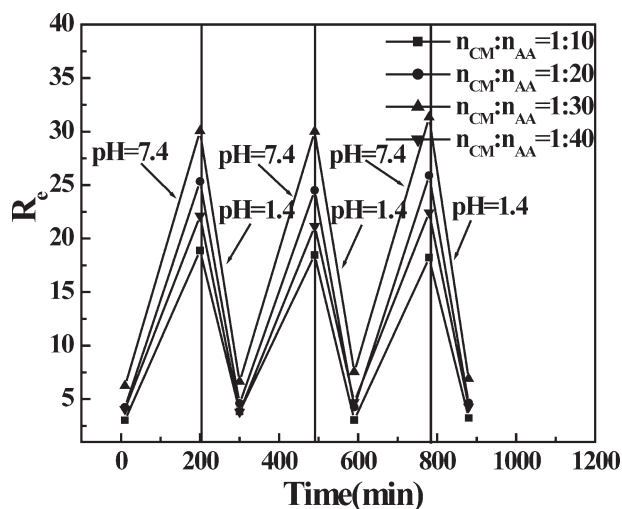
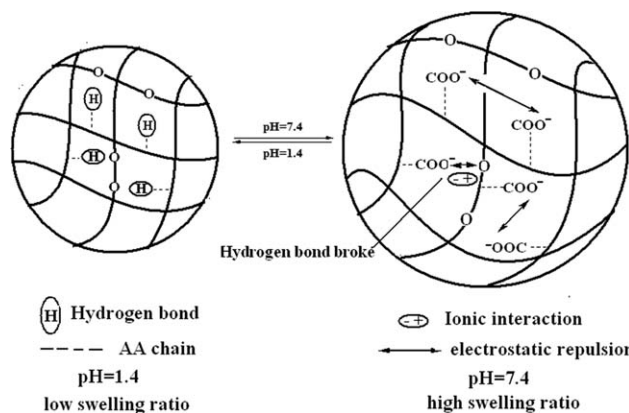
Theophylline Loading and Encapsulation Efficiency of Gels

The LE and EE of theophylline on P(AA-co-C₈PhEO₁₀Mac) gel were shown in Table III. It is found from the determinations that the introduction of an increase ratio of C₈PhEO₁₀Mac to AA, the LE of theophylline of hydrogels increased with increase ratio of C₈PhEO₁₀Mac to AA. It is may be attributed to the more porous structure (Figure 10).²⁷ In this work, the drug was not chemically attached to the polymer and the only likely interactions are electrostatic attraction and entrapment within the polymer matrix. Therefore, the drug should remain in a

biologically active form and could perform its function once released from the polymer matrix. Obviously, the major advantage of this formulation is that the drug in the polymer matrix is unaltered, and hence the efficacy of the released drug should be close to that of its native form.

Drug Delivery Studies

Drug release kinetics of P(AA-co-C₈PhEO₁₀Mac) hydrogels with different compositions were conducted at 37°C, and the effect in SGF and in SIF on the theophylline release was studied. In order to examine the *in vitro* drug release well, cumulative release is simultaneously presented in Figure 8 and Scheme 2. With regard to different release environments, it can be noticed that the release rate of theophylline slows up in the order of SIF and SGF, further denoting fast diffusion rate corresponding to matrix swelling and salt effects. It is also found from the determinations that the

**Figure 7.** Reversible swelling of the P(AA-co-C₈PhEO₁₀Mac) in buffers with pH of 1.4 and 7.4 at 37°C (Mean ± SD, $n = 3$).**Scheme 1.** Schematic illustration of the swelling behavior of pH-sensitive P(AA-co-C₈PhEO₁₀Mac) at different pH.**Table III.** Results of Loading Efficiency and Encapsulation Efficiency for Various Gels (Mean ± SD, $n = 3$ pH = 7.4)

$n_{CM}:n_{AA}$	Loading efficiency (%)	Encapsulation efficiency (%)
1:10	9.00	71.42
1:20	12.31	76.43
1:30	18.33	80.51
1:40	12.02	84.65

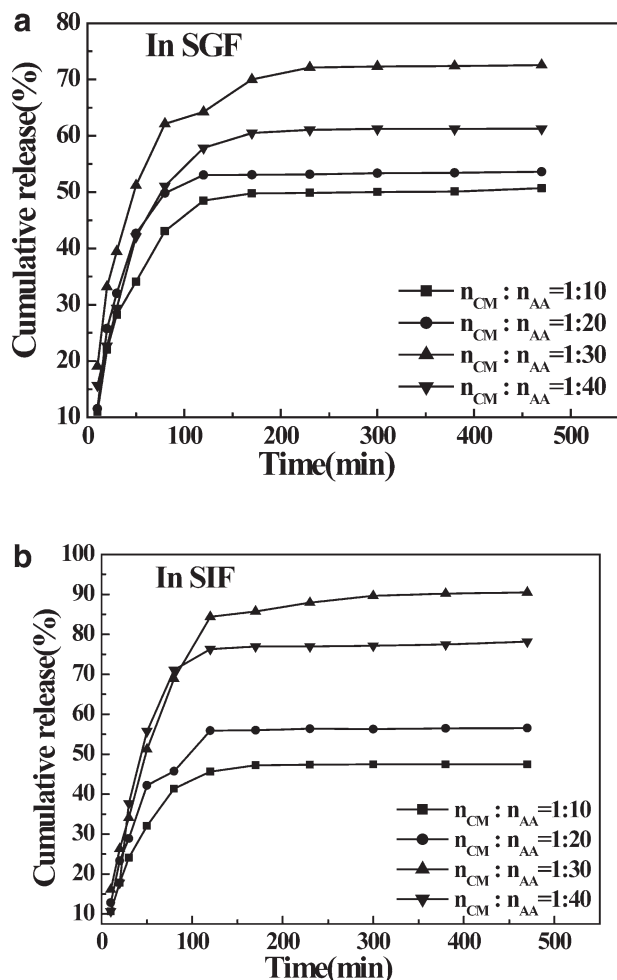
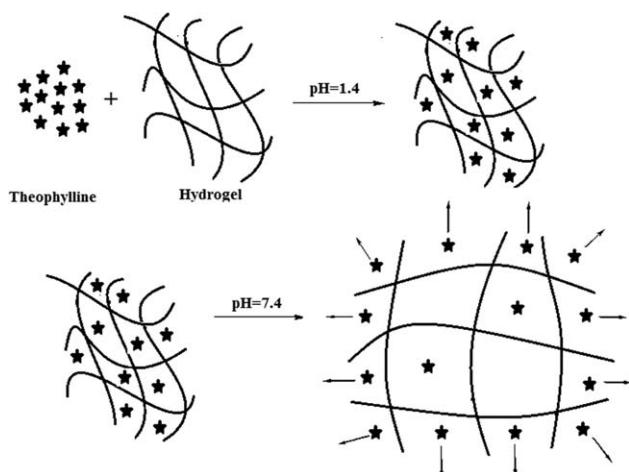


Figure 8. Theophylline release profiles for synthesized P(AA-co-C₈PhEO₁₀Mac) hydrogel at 37°C in SGF (a) and SIF (b) (means ± SD, *n* = 3).

introduction of an increase ratio of C₈PhEO₁₀Mac to AA, the cumulative release of hydrogels increased first and then decreased, when the ratio of C₈PhEO₁₀Mac to AA was 1:30, the cumulative



Scheme 2. Schematic drug diffusional illustration of theophylline loaded in P(AA-co-C₈PhEO₁₀Mac) hydrogel with different of solution media at pH = 1.4 and 7.4, respectively.

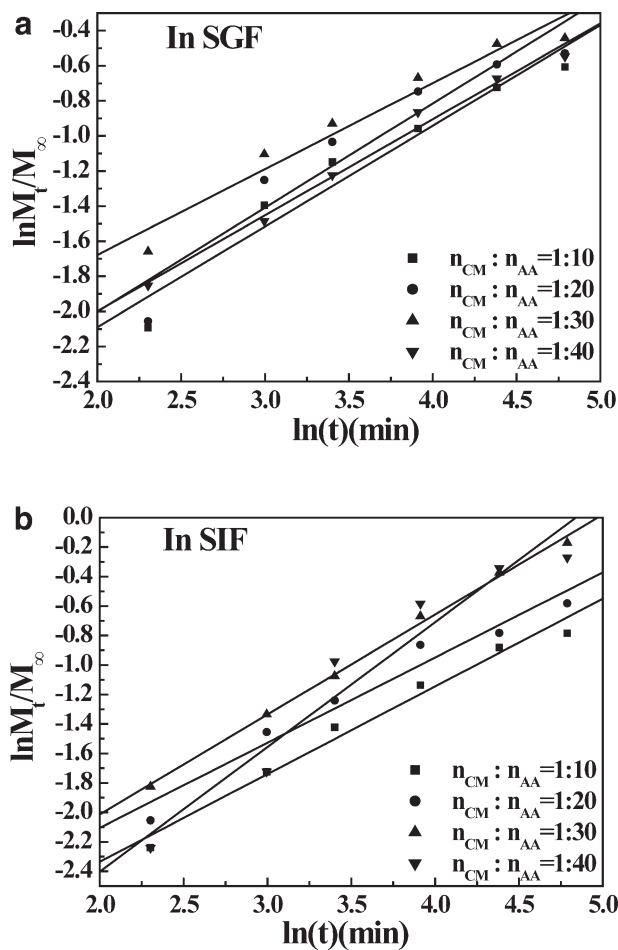


Figure 9. Linear regression curves of P(AA-co-C₈PhEO₁₀Mac) hydrogels containing different contents of hydrophobic C₈PhEO₁₀Mac units at two media (Mean ± SD, *n* = 3).

release was biggest. Correspondingly, the release time is greatly prolonged, indicating that the release of theophylline depends on not only the pH media, ionization ability, the matrix swelling, and salt effects, but also on the copolymer compositional ratios as well. Therefore, theophylline release, as can be expected, can be controlled or modulated by varying pH values, ionic strength as well as the ratios of copolymer chain units.

Dynamic swelling data of all the formulations have been fitted to an empirical eq. (8)²⁸:

$$\frac{M_t}{M_\infty} = kt^n \text{ or } \ln \frac{M_t}{M_\infty} = \ln k + n \ln t \quad (8)$$

According to eq. (8) and Figure 9, the relationship between $\ln(M_t/M_\infty)$ on $\ln(t)$ was made and the result is shown in Figure 9. After having been fitted, the kinetic parameters *k* and *n* as well as the correlation coefficient *R*² obtained are tabulated in Table IV. When *n* is less than or equal to 0.5, the drug release is controlled by Fickian diffusion mechanism. When the value of *n* is between 0.5 and 1, anomalous transport is observed. The preliminary kinetic modeling confirms that a new kind of intelligent hydrogel can be designed and created by a

Table IV. Regression Equations and Kinetic Parameters Obtained from fitting Drug Release Experimental Data to Ritger-Peppas Model (Mean \pm SD, $n = 3$)

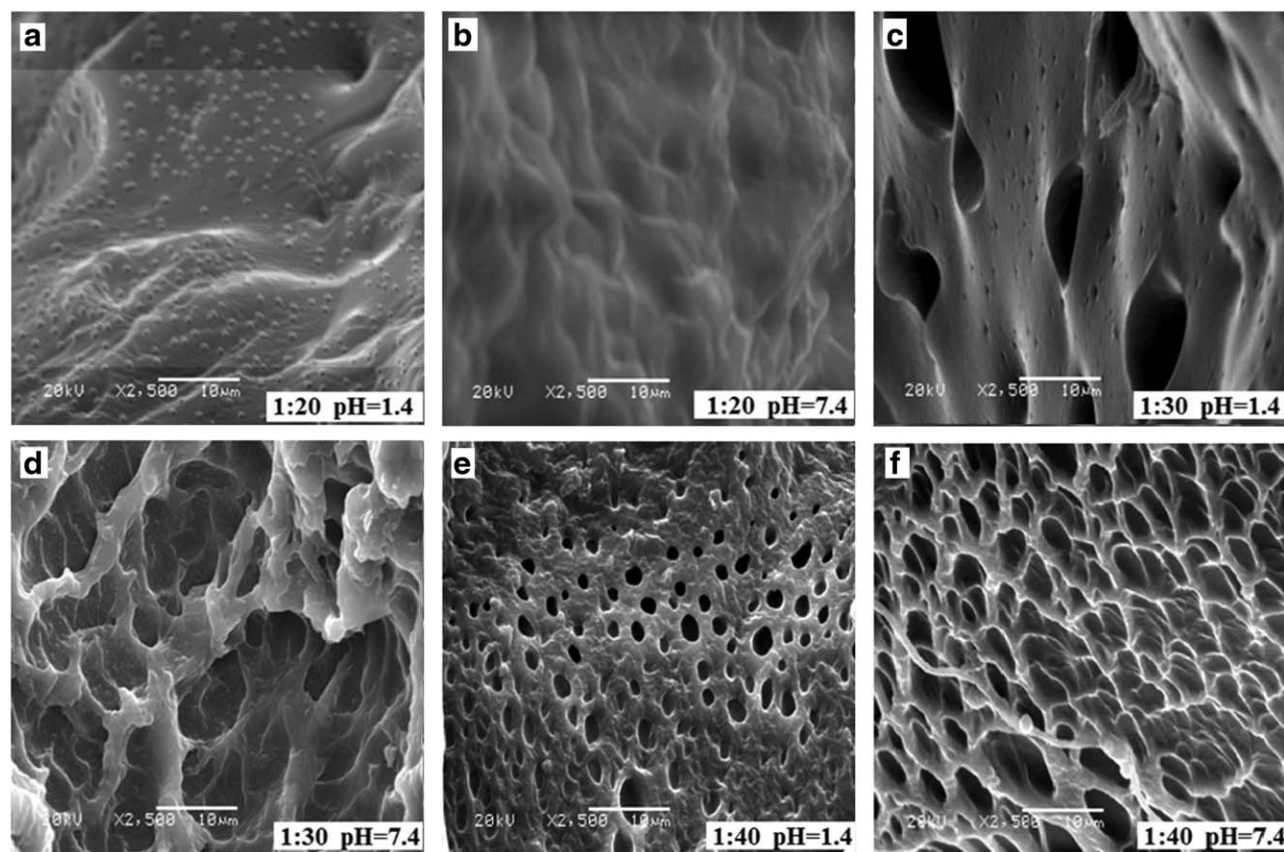
Medium	$n_{CM}:n_{AA}$	Regression equation	R^2	n	$\ln k$
SGF	1:10	$\ln(M_t/M_\infty) = 0.5242 \times -3.2386$	0.9542	0.5742	-3.2386
	1:20	$\ln(M_t/M_\infty) = 0.5932 \times -3.1880$	0.9100	0.5932	-3.1880
	1:30	$\ln(M_t/M_\infty) = 0.4896 \times -2.6577$	0.9512	0.4896	-2.6577
	1:40	$\ln(M_t/M_\infty) = 0.5470 \times -3.0932$	0.9882	0.5470	-3.0932
	1:10	$\ln(M_t/M_\infty) = 0.5951 \times -3.5352$	0.9802	0.5951	-3.5352
SIF	1:20	$\ln(M_t/M_\infty) = 0.5782 \times -3.2616$	0.9636	0.5782	-3.2616
	1:30	$\ln(M_t/M_\infty) = 0.6785 \times -3.3709$	0.9971	0.6785	-3.3709
	1:40	$\ln(M_t/M_\infty) = 0.8417 \times -4.0942$	0.9414	0.8417	-4.0942
	1:30	$\ln(M_t/M_\infty) = 0.6785 \times -3.3709$	0.9971	0.6785	-3.3709

hydrophobically modified route. Therefore the response of the hydrogels, the release rate, and the mode of the drug in various media can be modulated by adjusting the proportion of hydrophobic domains.^{29–31}

All curves in the figures are presented as average of three experiments. According to Figures 2–8, the swelling ratio, the equilibrium swelling ratio, and the cumulative release rate in stimulated intestinal fluids were higher than those in stimulated gastric fluids. With an increase of the content of AA, the swelling ratio, the equilibrium swelling ratio, and the cumulative release rate increased first and then decreased, when $n_{CM}:n_{AA}$ was 1:30, these quantities were biggest.

SEM Observations

The effect of the component ratios of $C_8PhEO_{10}Mac$ to AA and pH on the morphologies of $P(AA-co-C_8PhEO_{10}Mac)$ hydrogels is investigated, as shown in Figure 10. $P(AA-co-C_8PhEO_{10}Mac)$ hydrogels show a porous network structure, the macrostructure at pH 1.4 is seen to be compact compared with that in pH 7.4. Thus, in the acidic environment of the stomach, these microspheres are in a shrunken state, and protect drugs loaded inside. In the neutral and basic environments of the intestine, the microspheres are swollen thus allowing drugs to be released. In a basic SIF buffer solution, an electrostatic repulsion originated from the ionization of carboxyl groups causes breaking up of a

**Figure 10.** SEM micrographs of various $P(AA-co-C_8PhEO_{10}Mac)$ hydrogel samples in different pH.

number of hydrogen bonds and generates electrostatic repulsion among polymer chains, leading to the swelling of the hydrogel, and hence the polymer networks are stretched and are present as large porous structures. On the contrary, in the case of a SGF-stimulated environment, because of the existence of dissociative carboxylic acid groups in hydrogels, there existed a lot of hydrogen bonds in an acid medium, consequently, these hydrogen bond complex would restrict the movement or relaxation of network chains, and the network pores of P(AA-co-C₈PhEO₁₀-Mac) hydrogels contract, displaying relatively small micropores.

The results of SEM also show the morphological dependence on the AA content in the hydrogels. In fact, under the conditions of ratios of C₈PhEO₁₀Mac to AA below 1:40 [Figure 10(a–d)], with increasing in the AA content, their pore sizes increased, when the ratio was 1:30, the porosity was bigger, which is in agreement with the foregoing swelling results and drug release behavior variations (Figures 4 and 8). When the ratio was 1:40, a steric effect and a compartment effect of the three-dimensional network structures of hydrogels were obtained.

SEM findings reveal that the morphologies of the molecular pores of the hydrogels available for diffusion are dependent on the matrix swelling caused by environmental stimuli and monomer ratio, which effected on theophylline release.

CONCLUSIONS

A pH-sensitive hydrogel has been fabricated by free radical copolymerization of AA and C₈PhEO₁₀Mac in the presence of *N,N*-methylenebisacrylamide in this investigation. The experimental results have demonstrated that the gels do not swell greatly at low pH environments, whereas they can swell sufficiently at high pH solutions, exhibiting smart pH sensitivity. The swelling of P(AA-co-C₈PhEO₁₀Mac) hydrogels is also influenced by copolymer compositional ratio variables. This kind of swelling behavior is attributable to an electrostatic repulsion based on hydrogen bonding between the carboxylic acid groups, and an osmotic pressure between freely mobile ions within the gels and ions in buffer solutions. Considering the pH difference between the stomach and the intestines, this trait was expected to be used in the oral drug controlled release. It is interesting that the gels exhibited reversible response between pH 1.4 and 7.4. These results will be useful in designing and developing novel controlled delivery systems.

ACKNOWLEDGMENTS

This work was financially supported by the National Natural Science Foundation of China (21065010, 51262028) and the Key Laboratory of Polymer Materials of Gansu Province of China.

REFERENCES

1. Zhang, R.; Tang, M.; Bowyer, A.; Eisenthal, R.; Hubble, J. *Biomaterials* **2005**, *26*, 4677.
2. Nuttelman, C. R.; Rice, M. A.; Rydholm, A. E.; Salinas, C. N.; Shah, D. N.; Anseth, K. S. *Prog. Polym. Sci.* **2008**, *33*, 167.
3. Rokhade, A. P.; Agnihotri, S. A.; Patil, S. A.; Mallikarjuna, N. N.; Kulkarni, P. V.; Aminabhavi, T. M. *Carbohydr. Polym.* **2006**, *65*, 243.
4. Bardajee, G. R.; Pourjavadi, A.; Ghavami, S.; Soleyman, R.; Jafarpour, F. *J. Photochem. Photobiol. B* **2011**, *102*, 232.
5. Fan, T. F.; Li, M. J.; Wu, X. M.; Li, M.; Wu, Y. *Colloids Surf. B* **2011**, *88*, 593.
6. Chen, J.; Park, H.; Park, K. *J. Biomed. Mater. Res.* **1999**, *44*, 53.
7. Gemeinhart, R. A.; Park, H.; Park, K. *J. Biomed. Mater. Res.* **2001**, *55*, 54.
8. Serra, L.; Doménech, J.; Peppas, N. A. *Biomaterials* **2006**, *27*, 5440.
9. Luo, Y. F.; Peng, H.; Wu, J. C.; Sun, J. X.; Wang, Y. L. *Eur. Polym. J.* **2011**, *47*, 40.
10. Zhang, Y. X.; Wu, F. P.; Li, M. Z.; Wang, E. J. *Polymer* **2005**, *46*, 7695.
11. Xiao, Y. L.; Xu, W. J.; Zhu, Q. F.; Yan, B. F.; Yang, D.; Yang, F. J.; He, X. R.; Liang, S. C.; Hu, X. M. *Carbohydr. Polym.* **2009**, *77*, 612.
12. Vaghani, S. S.; Patel, M. M.; Satish, C. S. *Carbohydr. Res.* **2012**, *347*, 76.
13. Hezaveh, H.; Muhamad, I. I. *Int. J. Biol. Macromol.* **2012**, *50*, 1334.
14. Lin, W. C.; Yu, D. G.; Yang, M. C. *Colloids Surf. B* **2005**, *44*, 143.
15. Nita, L. E.; Chiriac, A. P.; Nistor, M. T.; Tartau, L. *Int. J. Pharm.* **2012**, *426*, 90.
16. Stubbe, B.; Maris, B.; Mooter, G. V.; De Smedt, S. C. J. *Demeester, J. Control. Rel.* **2001**, *75*, 103.
17. Castelli, F.; Sarpietro, M. G.; Micieli, D.; Ottimo, S.; Pitarresi, G.; Tripodo, G.; Carlisi, B.; Giammona, G. *Eur. J. Pharm. Sci.* **2008**, *35*, 76.
18. Oprea, A. M.; Profire, L.; Lupusoru, C. E.; Ghiciuc, C. M.; Ciolacu, D.; Vasile, C. *Carbohydr. Polym.* **2012**, *87*, 721.
19. Tefft, J. A.; Roskos, K. V.; Heller, J. *J. Biomed. Mater. Res. Part A* **1992**, *26*, 713.
20. Fundueanu, G.; Constantin, M.; Bortolotti, F.; Cortesi, R.; Ascenzi, P.; Menegatti, E. *Eur. J. Pharm. Biopharm.* **2007**, *66*, 11.
21. Fundueanu, G.; Constantin, M.; Esposito, E.; Cortesi, R.; Nastruzzi, C. *Biomaterials* **2005**, *26*, 4337.
22. Kajjari, P. B.; Manjeshwar, L. S.; Aminabhavi, T. M. *Ind. Eng. Chem. Res.* **2011**, *50*, 7833.
23. Gong, R. M.; Li, C. C.; Zhu, S. X.; Zhang, Y. Y.; Du, Y.; Jiang, J. H. *Carbohydr. Polym.* **2011**, *85*, 869.
24. Zhu, J. L.; Zhang, X. Z.; Cheng, H.; Li, Y. Y.; Cheng, S. X.; Zhuo, R. X. *J. Polym. Sci. Part A: Polym. Chem.* **2007**, *5*, 5354.
25. Luo, Y. L.; Wei, Q. B.; Xu, F.; Chen, Y. S.; Fan, L. H.; Zhang, C. H. *Mater. Chem. Phys.* **2009**, *118*, 329.
26. Luo, Y. L.; Zhang, K. P.; Wei, Q. G.; Liu, Z. Q.; Chen, Y. S. *Acta Biomater.* **2009**, *5*, 316.
27. Lin, W. C.; Yu, D. G.; Yang, M. C. *Colloids Surf. B: Biointerfaces.* **2005**, *44*, 143.
28. Soppimath, K. S.; Kulkarni, A. R.; Aminabhavi, T. M. *J. Biomater. Sci. Polym. Ed.* **2000**, *11*, 27.
29. Ritger, P. L.; Peppas, N. A. *J. Control. Rel.* **1987**, *5*, 23.
30. Higuchi, T. *J. Pharm. Sci.* **1963**, *52*, 1145.
31. Peppas, N. A.; Sahlin, J. J. *Int. J. Pharm.* **1989**, *57*, 169.